

This article was downloaded by:

On: 25 January 2011

Access details: *Access Details: Free Access*

Publisher *Taylor & Francis*

Informa Ltd Registered in England and Wales Registered Number: 1072954 Registered office: Mortimer House, 37-41 Mortimer Street, London W1T 3JH, UK



Journal of Liquid Chromatography & Related Technologies

Publication details, including instructions for authors and subscription information:

<http://www.informaworld.com/smpp/title~content=t713597273>

Thermo-Optical Spectroscopy: New and Sensitive Schemes for Detection in Capillary Separation Techniques

J. M. Saz^{ab}; J. C. Díez-Masa^c

^a Department of Analytical Chemistry Faculty of Science, Alcalá de Henares University, Madrid, Spain

^b Institute of Organic Chemistry (C.S.I.C.), ^c Institute of Organic Chemistry C.S.I.C. Juan de la Cierva, Madrid, Spain

To cite this Article Saz, J. M. and Díez-Masa, J. C.(1994) 'Thermo-Optical Spectroscopy: New and Sensitive Schemes for Detection in Capillary Separation Techniques', *Journal of Liquid Chromatography & Related Technologies*, 17: 3, 499 – 520

To link to this Article: DOI: 10.1080/10826079408013156

URL: <http://dx.doi.org/10.1080/10826079408013156>

PLEASE SCROLL DOWN FOR ARTICLE

Full terms and conditions of use: <http://www.informaworld.com/terms-and-conditions-of-access.pdf>

This article may be used for research, teaching and private study purposes. Any substantial or systematic reproduction, re-distribution, re-selling, loan or sub-licensing, systematic supply or distribution in any form to anyone is expressly forbidden.

The publisher does not give any warranty express or implied or make any representation that the contents will be complete or accurate or up to date. The accuracy of any instructions, formulae and drug doses should be independently verified with primary sources. The publisher shall not be liable for any loss, actions, claims, proceedings, demand or costs or damages whatsoever or howsoever caused arising directly or indirectly in connection with or arising out of the use of this material.

THERMO-OPTICAL SPECTROSCOPY: NEW AND SENSITIVE SCHEMES FOR DETECTION IN CAPILLARY SEPARATION TECHNIQUES

J. M. SAZ^{1*} AND J. C. DÍEZ-MASA²

¹*Department of Analytical Chemistry
Faculty of Science*

*Alcalá de Henares University
28801 Alcalá de Henares, Madrid, Spain*

²*Institute of Organic Chemistry
C.S.I.C.*

*Juan de la Cierva, 3
28006 Madrid, Spain*

ABSTRACT

Detection is a major problem in the application of Open-Tubular Capillary Liquid Chromatography (OTCLC) and Capillary Electrophoresis (CE) for analyzing very dilute samples, for instance in trace analysis. Thermo-optical Spectroscopy is a new branch of Spectroscopy which allows the detection of samples with low light absorbances (10^{-8} - 10^{-9} AU) using a few picoliters sample cell. A few attomoles of analyte can be detected in OTCLC or in CE with these techniques. These results are similar to those achieved by Laser-Induced Fluorescence detection in open-tubular capillary tubings. However, many organic substances present a high absorption coefficient and only a few of them provide good quantum yields. The principles of Thermo-optical Spectroscopy are presented in this work. The main thermo-optical methods and their application in OTCLC and CE are also reviewed.

**Temporarily assigned to Institute of Organic Chemistry (C.S.I.C.).*

INTRODUCTION

In recent years, capillaries whose internal diameter is increasingly smaller are being employed in Open-Tubular Capillary Liquid Chromatography (OTCLC) and Capillary Electrophoresis (CE) to contain the separation media (stationary phase, mobile phase or separation buffer). Capillary columns of a few micrometers of i.d. (5-10 μm) have been developed to be used as open-tubular capillary columns in HPLC. These columns allow the achievement of large efficiencies and short analysis time. Capillary tubes of 25 μm i.d. or smaller are being more frequently used in CE because of their excellent heat dissipation. However, such a reduction in i.d. requires the use of a very small volume (nL-pL) and mass (in the range of pg) of sample. Otherwise, efficiency loss and/or column overloading might occur. The use of such small samples is very demanding for other system components (injector, connexions, and detector) and prevent the analytical use of these techniques in trace analysis (ng/mL-pg/mL) due to detection limitations.

To illustrate the above detection problems using these capillary separation techniques in trace analysis, let's consider a sample volume of 1 nL (this is usually the maximum volume allowed in OTCLC and CE) with a trace level concentration of the solutes (1 ng/mL - 1 pg/mL) injected into the column. If we assume that the sample dilution is negligible during separation and consider that the volume of the detector cell should be around 1/10 of the peak volume to avoid efficiency losses, the detection limit for an analyte having a molecular weight of 100 a.m.u. should be 10^{-18} - 10^{-21} moles. For a conventional UV-Vis detector (1 cm path length) and an analyte with an absorption coefficient $\approx 10^3 \text{ AU} \times \text{cm}^{-1} \times \text{M}^{-1}$, this detection limit is equivalent to 10^{-5} AU. However, detection in OTCLC and CE must be on-column to prevent efficiency losses, which involves a great reduction in the optical path (capillary i.d. usually ranges from 5 to 100 μm in these separation techniques). This means that to use OTCLC and CE in trace analysis using conventional UV-Vis detection, a detection limit in the range of 1×10^{-7} - 0.5×10^{-9} AU is required. At the present time, the best commercial UV-Vis detectors for

these capillary separation techniques have detection limits approximately 10^{-4} - 10^{-5} AU.

There are only a few major possibilities to overcome the detection problem in trace analysis using capillary separation techniques: i) the use of sample preconcentration, particularly on-line techniques (1-4), ii) the pre-, on- or post-column sample derivatization (5), and iii) the use of high-sensitivity detection techniques. The on-line preconcentration can involve sample and efficiency losses and the hardship of finding a stationary phase to retain the analytes concerned. The sample derivatization can also involve efficiency losses (in post-column methodologies), and, in pre- and on-column derivatization, the appearance of some extra-peaks (derivatization agent, system peaks, etc) which make the analysis more complicated. The use of high-sensitivity detectors does not require sample manipulation, avoiding the above-mentioned problems. Since at the present time, spectroscopic methods present less problems for on-column detection, detection schemes employing this methodology are the most used in OTCLC and CE. From this viewpoint, those spectroscopic detection techniques whose response is proportional to the illuminating power (UV-Vis, Fluorescence, Phosphorescence, Photoionization, Photoconductivity, Thermo-optic and Thermo-acoustic techniques, etc) are especially appealing. The use of high illuminating power sources (e.g., laser radiation) in such detection techniques significantly improves their detection limits. Other spectroscopic methods whose response does not depend on the optical path (e.g., some thermo-optical methods) could be very interesting too for on-column detection in capillary separation techniques. Finally, detection schemes involving large optical paths which do not affect in a substantial manner the separation efficiency (e.g., UV-Vis Axial Detection (6)) could also be used in capillary separations.

The aim of this paper is to review the possibilities of the thermo-optical methods for detection in OTCLC and CE. In general terms, these methods can detect a very small sample absorbance (10^{-8} - 10^{-9} AU) in only a few picoliters of sample using an optical path in the range of micrometers. A few attomoles injected

into the capillary (7) could be monitored using these detectors, allowing the use of the OTCLC and CE in trace analysis. This sensitivity is similar to that obtained with Laser-Induced Fluorescence, but thermo-optical methods have a wider range of application because many substances absorb UV-Vis radiation and only a few present native fluorescence.

LASER PROPERTIES

The development of thermo-optical methods is associated to the laser unique properties, particularly its intensity (power per area unit) and coherence. Laser intensity is generally much larger than that of any other light source. This is very important in thermo-optical methods since there is a direct relationship between the illuminating power and the response obtained. However, due to the solvent absorbance, sample flow, and thermic effects, the noise also increases with the illuminating power and, hence, the signal/noise ratio increases up to a certain value and then remains constant.

The spatial and temporal coherence are related to the degree of correlation between the phases of any two points in the beam and the temporal variation of this correlation. Laser coherence is also higher than that of conventional illuminating sources. This feature allows focusing the beam within a very small spot size (a few micrometers radius), letting the design of detectors with very small sample cells (a few picoliters) and increasing detector response.

THE THERMO-OPTICAL EFFECT

All thermo-optical methods are based on the same principle: the Thermo-optical Effect. When a radiation beam with sufficient illuminating power (e.g., a laser) passes through a sample, it causes a temperature rise in the illuminated zone. This temperature rise is due to the light absorption of the analytes and the subsequent non-radiant relaxation of the originated species so that the temperature

increase is proportional to the sample absorbance. Such temperature rise causes a change in the refractive index of the sample transforming the illuminated zone in an optical element (a lens, a prism or a diffraction grating, depending on the beam transversal energy distribution). The characteristics of the thermo-optical elements are very sensitive to small absorbance changes and, therefore, thermo-optical methods can be used as high-sensitivity analytical techniques. Since there is a relationship between the thermo-optical element characteristics and the sample radiation absorbance, these thermo-optical elements can be used for detection in separation techniques and for quantitation purposes.

The response of thermo-optical methods depends on the thermo-optic effect intensity which, in turn, considerably depends on the solvent properties, particularly on the refractive index change with temperature (dn/dT) and thermic conductivity (k). The larger dn/dT and the smaller k , the larger the refractive index gradient is, the longer this gradient remains, and thus, the larger the thermo-optical response will be. Table 1 presents the dn/dT and k values for some solvents. It shows that non-polar solvents like Cl_4C are good solvents for thermo-optical techniques. Polar solvents (e.g., water) are the least appropriate for thermo-optical purposes due to their high k (however, if water is mixed with organic solvents as methanol or acetone its thermo-optical properties improve). Fluids at supercritical state like CO_2 (at 34 °C and 77 atm) are ideal solvents for thermo-optical techniques due to their large dn/dT .

In the following sections, the main thermo-optical methods, their principles, applications on OTCLC and CE detection, and detection limits will be described.

LASER-INDUCED INTERFEROMETRY

When a laser beam traverses a sample which absorbs the laser radiation, it causes a temperature rise and a concomitant refractive index decrease in the illuminated sample zone. The refractive index variation originates a phase change in the beam, and hence a change in the intensity of the interference beam obtained

TABLE 1

Thermo-optical properties of some solvents^a.

solvent	k (mW × cm ⁻¹ × K ⁻¹)	dn/dT × 10 ⁴ (K ⁻¹)
CO ₂ (34 °C y 77 atm)	0.95	-910
Cl ₄ C	1.03	-5.9
cyclohexane	1.24	-5.4
n-heptane	1.26	-5.0
acetone	1.60	-5.4
dioxane	1.39	-4.6
isobutyl alcohol	1.52	-3.9
methanol	2.02	-4.2
water	6.11	-0.8

^a Data from (41) and (42).

when recombined with another. The change in the interference beam intensity can be related to the sample absorbance.

The thermo-optical effect was first reported by Gordon et al (8), who described the relationship between the temperature increase $\Delta T(r, t)$ caused by a gaussian laser beam (as a function of the distance from the center of the irradiated zone r , and the irradiation time t) and the sample absorption coefficient (ϵ):

$$\Delta T(r, t) = \frac{\epsilon P}{16 \cdot 8 \pi k} \left[\ln(1 + 8Dt/\omega^2) - \frac{1}{(1 + \omega^2/8Dt)} \frac{2r^2}{\omega^2} \right] \quad (1)$$

(see Glossary for symbols).

The temperature increase is related to the refractive index variation (Δn) by:

$$\Delta n = \frac{\partial n}{\partial T} \Delta T \quad (2)$$

In turn, the refractive index change is related to the phase beam change ($\Delta\phi$) by:

$$\Delta\phi = 2\pi \frac{l}{\lambda} \Delta n \quad (3)$$

Finally, the phase change is related to the interference beam intensity (I_s):

$$I_s = \frac{1}{2} I_{\max} (1 + \cos \Delta\phi) \quad (4)$$

Equations 1 to 4 show a relationship between laser properties (P , λ and ω), sample characteristics (dn/dT , k and l), and signal produced (I_s). High power and short wavelength lasers tightly focused within the sample increase the signal. Samples with large temperature dependence of refractive index, small thermal conductivity, and long optical path also do.

Figure 1 shows a laser interferometer. The radiation from a He-Ne laser goes through an uncoated optical flat splitting the laser radiation in two beams (M and m) with different energy (M has much more energy than m). Both beams pass through the sample. M heats the sample producing a refractive index variation which causes a phase shift. The phase shift in m is negligible because it has low energy and almost no refractive index variation is originated in the sample region traversed by this beam. After passing across the sample, M goes through another uncoated optical flat and it is again divided in two beams (MM and Mm). Mm interferes with m producing an interference beam (mMm) whose intensity is related to the sample absorbance. MM is sent to a photodiode as reference signal.

Several laser-induced interferometry schemes have been described to determine small absorbance in static samples (9-12). Sample cells with several centimeters of optical path have been used in these schemes. To compare detection

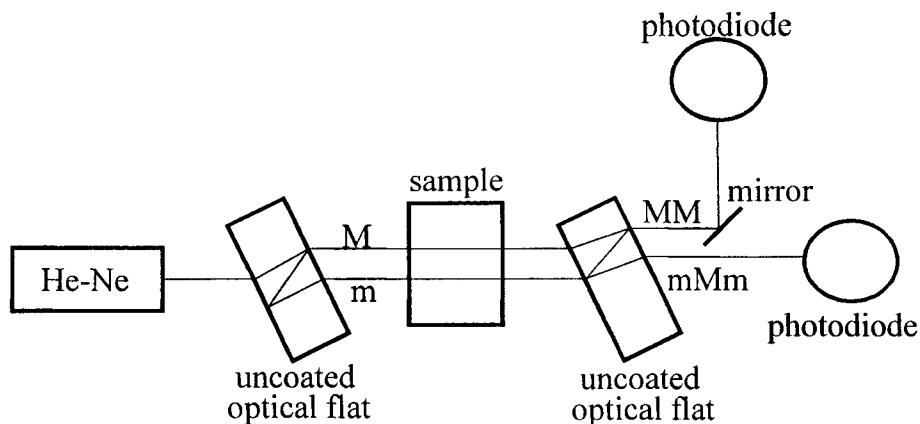


FIGURE 1. Jamin-laser interferometer. The laser beam from a He-Ne laser is splitted in two beams (M and m) with different energy (M has much more energy than m). Both of them go through the sample causing a different heating and refractive index change in the region traversed producing a phase shift between them. M is again splitted in two beams (MM and Mm), MM goes to the photodiode and is used as reference, and Mm is superimposed to m producing an interference signal that goes to another photodiode.

limits achieved with different cells, the sensitivity should be expressed as the ϵC product (absorbance per optical path unit). Detection limits in the range of 10^{-5} - 10^{-6} $\text{AU} \times \text{cm}^{-1}$ were obtained (13).

These laser-based interferometers have also been used as detectors in liquid chromatography (packed, 4.6 mm i.d. columns). Employing 1 cm path length sample cells, a detection limit of 2.6×10^{-6} AU was obtained (14).

LASER-INDUCED THERMAL LENS SPECTROSCOPY

When a laser beam with sufficient power and a gaussian distribution of energy (TEM_{00}) traverses a sample region, it generates a gaussian temperature distribution and, therefore, a gaussian refractive index distribution in the region

illuminated. Since the temperature value in the center of the illuminated zone is the highest, the refractive index value at the center of this zone is the lowest and this value increases radially along the sample. Consequently, the illuminated zone behaves as a divergent lens for any beam which traverses it. The focal distance (f) of such a lens is related to the sample absorbance (A) (15) according to the equation:

$$\frac{1}{f} = \frac{2.03P(dn/dT)A}{\pi k \omega^2} \quad (5)$$

The divergence originated by the thermal lens produces an increase in the section area of the beam and, because the total beam energy is constant, it causes a drop in the illuminating intensity at the beam center. Therefore, the intensity change at the beam center can be related to the sample absorbance. When the sample is placed at the position $\sqrt{3}z_c$ behind the beam waist, the equation proposed by Carter and Harris (15) relates the intensity change to the sample absorbance:

$$\frac{I_o - I}{I_o} = 2.303EA + \frac{(2.303EA)^2}{2} \quad (6)$$

Where E is defined as:

$$E = -\frac{P(dn/dT)}{1.91\lambda k} \quad (7)$$

Equations 6 and 7 show that the signal originated by the thermal lens is proportional to the sample absorbance and the E factor. The E factor can be considered as an increment factor of the thermal lens signal when compared to conventional UV-Vis spectroscopy signal (A). This increment depends on the laser power (P), laser wavelength (λ), the variation of the sample refractive index with temperature (dn/dT), and sample thermal conductivity (k). An increase in the intensity change ($I_o - I/I_o$) can be achieved for the same sample by increasing the laser power (P).

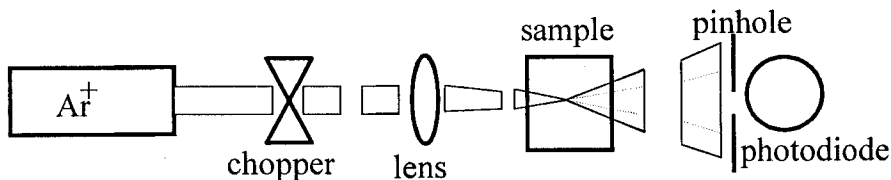


FIGURE 2. Single-beam thermal lens spectrophotometer. The laser beam from a laser source with sufficient power to produce the thermo-optical effect (e.g., a Ar^+ laser) is modulated by a chopper and focused by a lens within the sample producing a divergent thermal lens which increases the beam section and decreases its intensity at the center, being detected by a photodiode through a pinhole.

Several thermal lens spectroscopy schemes have been described. Figure 2 shows the simplest arrangement based on a single laser beam with sufficient power to produce the thermal lens effect. The beam is modulated with a chopper so that the thermal lens is intermittently formed and dissipated. Data on the beam center intensity is periodically obtained before and after lens formation.

The noise decreases and, therefore, detection limit improves by using two lasers (16) (Figure 3). A pump laser (e.g., Ar^+), with high power and low stability to produce the thermal lens effect and a probe laser (e.g., He-Ne), with low power and larger stability (whose intensity change are measured after passing through the thermal lens), are used in this technique. The pump laser is modulated with a chopper. Using a mirror and a beam splitter, the pump and probe beams are superimposed; a filter before the photodiode blocks the pump beam radiation.

The detection limits achieved using thermal lens spectroscopy in static samples (detection cells with 1 cm or more optical paths) are in the range of 10^{-7} - 10^{-8} $\text{AU} \times \text{cm}^{-1}$ (17). Thermal lens spectroscopy has also been used for detection in liquid chromatography with packed columns (1 mm and 4.6 mm i.d.) (18-20) as well as in open-tubular capillaries (20 μm i.d.) (21). The detection limit obtained in liquid chromatography using 20 μm i.d. capillaries has been 9×10^{-5} AU ($\epsilon\text{C} \approx 9 \times 10^{-3}$ $\text{AU} \times \text{cm}^{-1}$) (21).

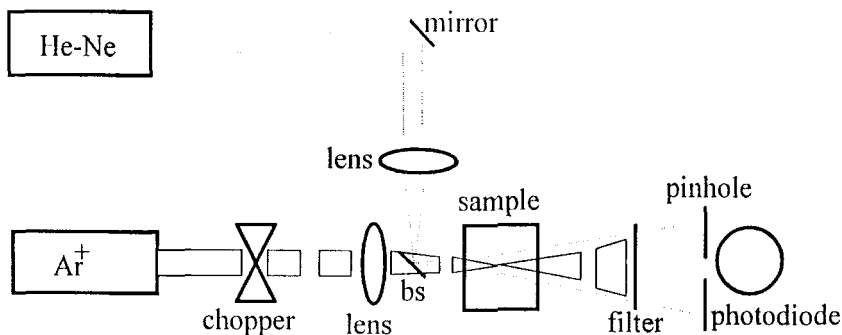


FIGURE 3. Coaxial-beam thermal lens spectrophotometer. The laser beams from two laser sources illuminate coaxially the sample. One of the lasers is modulated and has sufficient power to produce the thermal lens effect (Ar^+ laser), the other has high stability to decrease the noise (He-Ne laser) and probes the thermal lens undergoing a section increase and an intensity drop at its central point, which can be detected by a photodiode. The filter blocks the Ar^+ laser beam radiation.

Another thermal lens setup uses two orthogonally crossed beams instead of coaxial beams (Figure 4). The thermo-optical element behaves as a cylindrical lens which produces a beam divergence related to the sample absorbance. Since the true optical path is reduced to the crossing volume of the pump and probe beams, a high spatial resolution (small illuminated volume) in the sub-picoliter range (22) and a signal not depending on the virtual optical path (sample cell thickness) have been obtained. These features make the crossed-beam thermal lens spectroscopy suitable as a detection system in capillary separation techniques.

The mathematical model for crossed-beam thermal lens spectroscopy has been developed (23) for a pulsed pump laser, but it can be easily adapted to a continuous or modulated pump laser. This model relates the change in relative intensity at the probe beam center ($I_t - I_o / I_o$) to the sample absorption coefficient (ϵ) and sample concentration (C):

$$\frac{I_t - I_o}{I_o} = \frac{\theta \epsilon C / t_c}{(1 + 2t / t_c)^{3/2}} \quad (8)$$

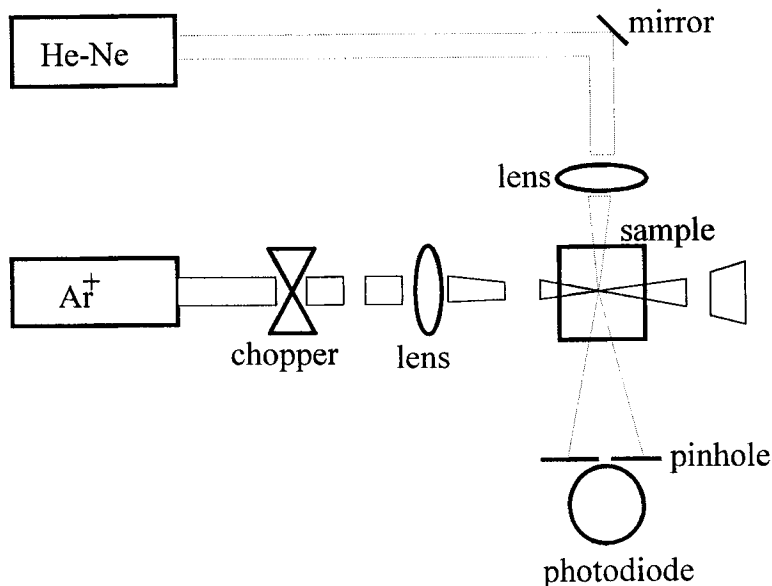


FIGURE 4. Crossed-beam thermal lens spectrophotometer. The thermo-optical element produced by a modulated Ar⁺ laser beam behaves as a cylindrical lens generating a divergence in the He-Ne laser beam detected by the photodiode.

Where:

$$\theta = \frac{4.606 \epsilon C (dn/dT) z_1}{(2\pi)^{1/2} \omega_c k} \quad (9)$$

and t_c is a constant related to thermo-optical element relaxation time, defined as:

$$t_c = \frac{\omega_c C}{4kp} \quad (10)$$

Using orthogonally crossed-beam techniques, the detection limits obtained in static samples are $\sim 10^{-9}$ AU with optical paths of $\sim 3 \mu\text{m}$ (24). This means a detection limit of 1-2 orders of magnitude smaller than those obtained using coaxial beams thermal lens arrangements (10^{-7} - 10^{-8} AU), with a detection volume in the sub-picoliter range.

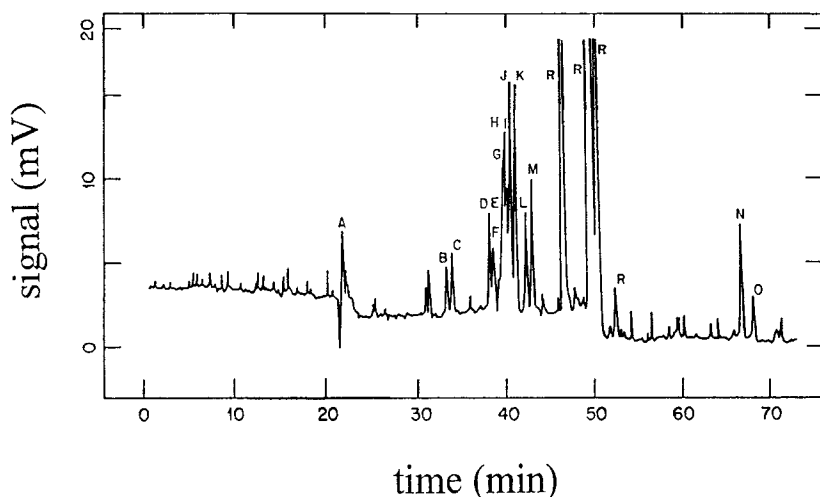


FIGURE 5. Electropherogram of DABSYL-amino acids using crossed-beam thermal lens detection. 2.5×10^{-6} M solution injected, at 5 kV for 5 s, corresponding to 0.7 nL and 1.7 fmol of each amino acid approximately. A, arginine; B, histidine; C, lysine; D, cysteine and tyrosine; E, tryptophan; F, proline; G, phenylalanine; H, leucine; I, methionine; J, isoleucine and valine; K, tyrosine and serine; L, alanine; M, glycine; R, reagent peaks; N, glutamic acid; O, aspartic acid. Reproduced from reference (7) with permission of the American Chemical Society.

Crossed-beam thermal lens spectroscopy has been applied to detection in separation techniques using microbore columns (0.25 - 1 mm i.d.) (25-27), and capillary columns (50 - 200 μ m i.d.) (7,28). The detection limit obtained in all cases was in the range of 10^{-7} AU despite the cell thickness was different in each case. Detection limits of 37 attomoles injected into a capillary electrophoresis column have been obtained using 4-(dimethylamino)azobenzene-4'-sulfonyl chloride derivatized amino acids (DABSYL-amino acids) (7). This result is similar to the best results obtained in fluorescent detection using derivatized amino acids (29-30). Figure 5 shows an electropherogram of several DABSYL-amino acids separated by capillary electrophoresis (50 μ m i.d.) using crossed-beam thermal lens spectroscopy detection.

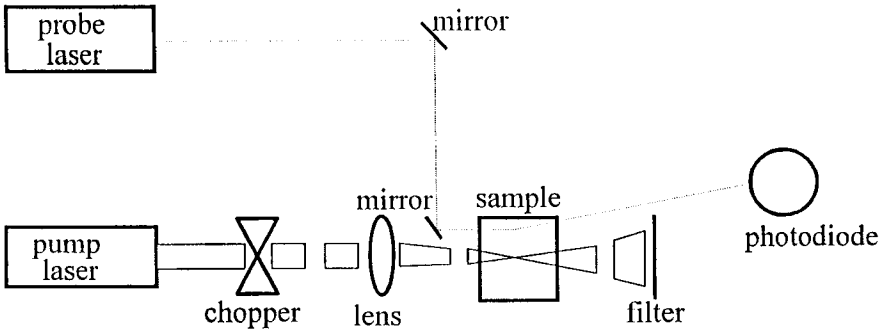


FIGURE 6. Thermal prism spectrophotometer. A modulated pump beam produces a thermal lens within the sample, and a probe laser traverses it close to the thermal lens border originating a beam deflection detected by a position-sensitive photodiode.

LASER-INDUCED THERMAL PRISM SPECTROSCOPY

In this thermo-optical technique, a laser beam with a gaussian energy distribution illuminates the sample, but the probe beam passes through a region close to the thermal lens border instead of through its center as in thermal lens techniques. In this way, the thermal element behaves as an optical prism deflecting the beam (Figure 6). Although the deflection amplitude is very small (10^{-8} - 10^{-9} rad), it can be measured and related to the sample absorbance (31).

The theoretical model proposed by Boccara et al (31) is based on the assumption that the sample behaves as an optical prism. The equations of this model relate the beam deflection (ψ) to the sample absorption coefficient (ϵ). If the thermic gradient radius in the sample is smaller than the pump beam radius (e.g., using high modulation frequencies in the pump beam or pulsed pump lasers), then:

$$\psi = \frac{P_o (dn/dT)}{\nu \rho c \pi^2 \omega_o^2} [1 - \exp(-\epsilon l)] \left[-\frac{2x_o}{\omega_o} \exp\left(-\frac{x_o^2}{\omega_o^2}\right) \right] \quad (11)$$

But if the sample thermal diffusion is larger than the pump beam radius, then:

$$\psi = \frac{P_o (dn/dT)}{k\kappa^2 x_o} [1 - \exp(-\epsilon l)] [1 - \exp(-\frac{x_o^2}{\omega_o^2})] \quad (12)$$

According to these equations, the response of this technique (ψ) depends on the pump laser power (P_o) and radius (ω_o), the sample thermo-optical properties (dn/dT and k), and the distance (x_o) between pump and probe beam centers.

The detection limits obtained in static samples using detection cells of 100 μm thickness are around 10^{-8} AU (32). The thermal prism spectroscopy has also been used for liquid chromatography detection using microbore columns (1 mm i.d.). In this case, a detection limit of 3×10^{-8} AU was achieved (33).

LASER-INDUCED THERMAL DIFFRACTION GRATING SPECTROSCOPY

If a laser beam is splitted in two beams which are subsequently crossed with a given angle within the sample, it causes a fringe interference pattern and, therefore, a similar fringe pattern in the sample refractive index (Figure 7). In this case, the illuminated zone generates a diffraction grating. The fringe spacing (d) depends on the laser wavelength (λ_o) and the crossing angle (θ_o) (referred to the bisectrix of both beams) according to Bragg's law:

$$d = \frac{\lambda_o}{2\sin\theta_o} \quad (13)$$

Equation 13 shows that the fringe spacing can be modified by changing the beams' crossing angle. When this spacing is much smaller than the fringe thickness, the thermo-optical element behaves as a Bragg diffraction grating. If a probe beam intersects this grating at Bragg's angle ($\theta_b = 2\sin^{-1}(\lambda_p/2d)$), the intensity of the diffracted radiation (I_d) is related to the sample absorption

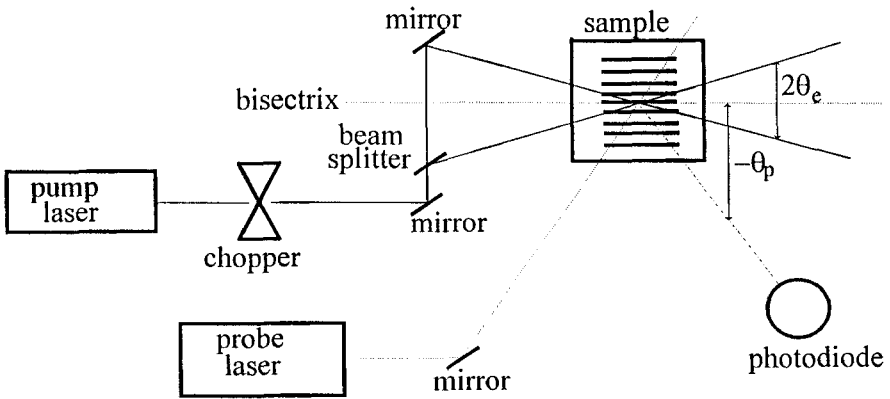


FIGURE 7. Thermal diffraction grating spectrophotometer. The laser beam from a modulated pump laser is splitted in two beams which are crossed within the sample causing a fringe interference pattern on the sample refractive index. This thermo-optical element diffracts the probe beam behaving as a diffracted grating. The intensity of the diffracted beam is measured by a photodiode.

coefficient (ϵ) and sample concentration (C) by:

$$\frac{I_d}{I_o} = \frac{8\pi}{3^{1/2}} \left[\frac{2 \cdot 303 E_p (dn/dT) \epsilon C}{\rho c \omega_e \lambda_p \sin(2\theta_b)} \right]^2 \quad (14)$$

The sample volume is defined by the pump and probe beams intersection like in crossed-beam thermal lenses. Hence, this volume can be very small and, consequently, the signal is independent of the real sample cell size. Equation 14 also shows an inverse and quadratic relationship between the true optical path (ω_e) and the interference signal. It also shows a quadratic relationship between the signal and pump beam energy (E_p) and the sample concentration (C), demonstrating the potential that thermal grating has as a high-sensitivity detection technique.

A minimum number of fringes (10 to 20) is necessary to obtain a signal intense enough. In practice, this makes sample volumes in thermal gratings (nL)

not as small as in crossed-beam thermal lens spectroscopy (pL). The instrumentation alignment in a thermal grating setup is more strict than in the other thermo-optical methods. Small alignment changes (in the order of one thousandth of degree) produce large signal variations.

The detection limits for this technique in static samples are in the range of 10^{-7} AU (34). However, to the best of our knowledge, this technique has not been applied in OTCLC or CE detection yet.

POTENTIALS AND LIMITATIONS OF THERMO-OPTICAL METHODS APPLIED TO OTCLC AND CE DETECTION

One of the thermo-optical detection problems limiting the technique sensitivity is the noise. The instability of the laser intensity (for continuous pump lasers normally used in Thermo-optical Spectroscopy approximately 1%) is the primary cause of this noise. This instability is two orders of magnitude larger than that of a good conventional (non-coherent) light source. The use of laser stabilizers reduces the laser noise up to 0.1 %. The two laser arrangements (for pumping and probing the sample) (16), and/or the use of reference channels to compensate the source fluctuations (35) can also reduce the noise.

The thermo-optical element dissipation due to the mobile phase flow which decreases the signal amplitude is another problem. The use of pulsed lasers (36,37), continuous lasers with high modulation frequencies (38), and focusing of the probe beam slightly down the pump beam (39), decrease the dissipation effect caused by the flow rate producing more intense signals .

A further limitation for using thermo-optical methods as routine detection in capillary separation techniques is associated with the small internal diameter of the capillaries used (40). This effect can originate a beam section deformation when it passes through the capillary, a beam deflection when it is not symmetrically focused on the capillary axis, and a complicated interference patterns if the beam size and the capillary i.d. are similar.

On the other hand, Thermo-optical Spectroscopy is a promising technique for OTCLC and CE detection despite only a few applications have been described in this field to date. Crossed-beam thermo-optical techniques are particularly promising for their high sensitivity (detection limit in the range of 10^{-9} AU), small probing volume (in the sub-picoliter range), and virtual non-path length dependence of the response. The sensitivity obtained by some thermo-optical techniques could allow the use of OTCLC and CE in trace analysis. However, thermo-optical methods are not yet being used on a routine basis for detection in capillary separation techniques. The pump lasers' high cost, the lack of tunable lasers in most of the UV range, and the skill required to design good thermo-optical setups, may be some of the reasons for the restricted use of these techniques. The progress in laser technologies nowadays (tunable lasers, diode lasers, etc.) will allow a more routinary use of thermo-optical methods as detection techniques in OTCLC and CE in a near future.

ACKNOWLEDGEMENTS

The authors thank DGICYT for granting project PB-88-034 on Capillary Electrophoresis Detection which has made this work possible.

GLOSSARY

- A*: sample absorbance.
- C*: analyte sample concentration.
- c*: sample specific heat capacity.
- D*: analyte diffusion coefficient.
- d*: fringe spacing in thermal grating spectroscopy.
- E*: response increment factor in thermal lens spectroscopy.
- E_e*: pump beam energy.
- f*: thermal lens focal distance.
- I*: probe beam intensity after passing through the thermo-optical element.
- I_d*: diffracted probe beam intensity in thermal grating spectroscopy.
- I_{max}*: signal maximum intensity in laser interferometry.
- I₀*: probe beam intensity prior to thermo-optical element formation.
- I_s*: signal intensity in laser interferometry.
- I_t*: probe beam intensity after passing through the thermo-optical element at

a	given time t .
k	sample thermic conductivity.
l	sample cell thickness.
n	sample refractive index.
Δn	sample refractive index change.
P	laser beam power.
P_c	pump beam power.
r	position of any point anywhere in the beam referred to section center.
T	sample temperature.
ΔT	change in sample temperature.
t	time.
t_c	constant related to the thermo-optical element relaxation time.
x_o	distance between the pump and probe beam centers in thermal prism spectroscopy.
z_c	confocal distance; distance between the beam waist and the point for what beam section is double than beam waist section.
z_l	distance between the probe beam waist and beams' crossing point in crossed-beam thermal lens spectroscopy.
ϵ	sample absorption coefficient.
θ_b	Bragg's angle.
θ_c	angle between pump beams and their bisectrix in thermal grating spectroscopy.
θ_p	angle between probe beam and pump beams bisectrix in thermal grating spectroscopy.
λ	laser beam wavelength.
λ_c	pump beam wavelength.
λ_p	probe beam wavelength.
ν	pump beam modulation frequency.
ρ	sample density.
$\Delta\phi$	change in the probe beam phase in laser interferometry.
ψ	probe beam deflection in thermal prism spectroscopy.
ω	laser beam radius in the sample.
ω_c	pump beam radius in the sample.

REFERENCES

- (1) M. Goto, T. Takeuchi and D. Ishii, *Adv. Chromatogr.*, **30**: 167 (1989).
- (2) F. Foret, E. Szoko and B.L. Karger, *J. Chromatogr.*, **608**: 3 (1992).
- (3) M. Merion, R.H. Aebersold and M. Fuchs, 3rd Int. Symp. on High Performance Capillary Electrophoresis, San Diego, 1991.

- (4) R.L. Chien and D.S. Burgi, *Anal. Chem.*, **64**: 489A (1992).
- (5) D.F. Swaile and M.J. Sepaniak, *J. Liq. Chromatogr.*, **14**: 869 (1991).
- (6) E.S. Yeung, *J. Chin. Chem. Soc.*, **38**: 307 (1991).
- (7) M. Yu and N.J. Dovichi, *Anal. Chem.*, **61**: 37 (1989).
- (8) J.P. Gordon, R.C.C. Leite, R.S. Moore, S.P.S. Porto and J.R. Whinnery, *J. Appl. Phys.*, **36**: 3 (1965).
- (9) J. Stone, *J. Opt. Soc. Am.*, **62**: 327 (1972).
- (10) J. Stone, *Appl. Opt.*, **12**: 1828(1973).
- (11) L. Skolnik, A. Hordvik and A. Kahan, *Appl. Phys. Lett.*, **23**: 477 (1973).
- (12) A. Hordvik, *Appl. Opt.*, **16**: 2827 (1977).
- (13) D.A. Cremers and R.A. Keller, *Appl. Opt.*, **21**: 1654 (1982).
- (14) S.D. Woodruff and E.S. Yeung, *Anal. Chem.*, **54**: 1174 (1982).
- (15) C.A. Carter and J.M. Harris, *Anal. Chem.*, **56**: 922 (1984).
- (16) M.E. Long, R.L. Swofford and A.C. Albrecht, *Science*, **191**: 183 (1976).
- (17) N.J. Dovichi and J.M. Harris, *Anal. Chem.*, **53**: 106 (1981).
- (18) R.A. Leach and J.M. Harris, *J. Chromatogr.*, **218**: 15 (1981).
- (19) C.E. Buffett and M.D. Morris, *Anal. Chem.*, **54**: 1824 (1982).
- (20) C.E. Buffett and M.D. Morris, *Anal. Chem.*, **55**: 378 (1983).
- (21) M.J. Sepaniak, J.D. Vargo, C.N. Kettler and M.P. Maskarinec, *Anal. Chem.*, **56**: 1252 (1984).
- (22) T. G. Nolan, W.A. Weimer and N.J. Dovichi, *Anal. Chem.*, **56**: 1704 (1984).
- (23) N. J. Dovichi, T.G. Nolan and W.A. Weimer, *Anal. Chem.*, **56**: 1700 (1984).

- (24) T. G. Nolan and N.J. Dovichi, *IEEE Circuits Devices Mag.*, 2: 54 (1986).
- (25) T.G. Nolan, B.K. Hart and N.J. Dovichi, *Anal. Chem.*, 57: 2703 (1985).
- (26) T.G. Nolan, D.J. Bornhop and N.J. Dovichi, *J. Chromatogr.*, 384: 189 (1987).
- (27) T.G. Nolan and N.J. Dovichi, *Anal. Chem.*, 59: 2803 (1987).
- (28) C.N. Kettler and M.J. Sepaniak, *Anal. Chem.*, 59: 1733 (1987).
- (29) S. Einarsson, S. Folestad, B. Josefsson and S. Lagerkvist, *Anal. Chem.*, 58: 1638 (1986).
- (30) P. Gozel, E. Gassmann, H. Michelsen and R.N. Zare, *Anal. Chem.*, 59: 44 (1987).
- (31) A.C. Boccara, D. Fournier, W.J. Jackson and N.M. Amer, *Opt. Lett.*, 5: 377 (1980).
- (32) W.B. Jackson, N.M. Amer, A.C. Boccara and D. Fournier, *Appl. Opt.*, 20: 1333 (1981).
- (33) T.W. Collette, N.J. Parekh, J.H. Griffin, L.A. Carreira and L.B. Rogers, *Appl. Spectrosc.*, 40: 164 (1986).
- (34) D.J. McGraw and J.M. Harris, *J. Opt. Soc. Am.*, B 2: 1471 (1985).
- (35) N.J. Dovichi and J.M. Harris, *Anal. Chem.*, 51: 728 (1979).
- (36) S.L. Nikolaisen and S.E. Bialkowski, *Anal. Chem.*, 57: 758 (1985).
- (37) S.L. Nikolaisen and S.E. Bialkowski, *Anal. Chem.*, 58: 215 (1986).
- (38) K.J. Skogerboe and E.S. Yeung, *Anal. Chem.*, 58: 1014 (1986).
- (39) W.A. Weimer and N.J. Dovichi, *Anal. Chem.*, 57: 2436 (1985).
- (40) A.E. Bruno, A. Paulus and J. Bornhop, *Appl. Spectrosc.*, 45: 462 (1991).

- (41) J.M. Harris, *Optics News*, oct: 8 (1986).
- (42) B.G. Belenkii, *J. Chromatogr.*, 434: 337 (1988).

Received: April 10, 1993

Accepted: August 2, 1993